



Published in final edited form as:

*Nat Ecol Evol.* ; 1(5): 126. doi:10.1038/s41559-017-0126.

## Contentious relationships in phylogenomic studies can be driven by a handful of genes

Xing-Xing Shen<sup>1</sup>, Chris Todd Hittinger<sup>2</sup>, and Antonis Rokas<sup>1,\*</sup>

<sup>1</sup>Department of Biological Sciences, Vanderbilt University, Nashville, TN 37235, USA

<sup>2</sup>Laboratory of Genetics, Genome Center of Wisconsin, DOE Great Lakes Bioenergy Research Center, Wisconsin Energy Institute, J. F. Crow Institute for the Study of Evolution, University of Wisconsin-Madison, Madison, WI 53706, USA

### Abstract

Phylogenomic studies have resolved countless branches of the tree of life (ToL), but remain strongly contradictory on certain, contentious relationships. Here, we employ a maximum likelihood framework to quantify the distribution of phylogenetic signal among genes and sites for 17 contentious branches and 6 well-established control branches in plant, animal, and fungal phylogenomic data matrices. We find that resolution in some of these 17 branches rests on a single gene or a few sites, and that removal of a single gene in concatenation analyses or a single site from every gene in coalescence-based analyses diminishes support and can alter the inferred topology. These results suggest that tiny subsets of very large data matrices drive the resolution of specific internodes, providing a dissection of the distribution of support and observed incongruence in phylogenomic analyses. We submit that quantifying the distribution of phylogenetic signal in phylogenomic data is essential for evaluating whether branches, especially contentious ones, are truly resolved. Finally, we offer one detailed example of such an evaluation for the controversy regarding the earliest-branching metazoan phylum, where examination of the distributions of gene-wise and site-wise phylogenetic signal across 8 data matrices consistently supports ctenophores as sister group to all other metazoans.

### Keywords

Phylogenetics; Conflict; Incongruence; Gene Tree

---

Users may view, print, copy, and download text and data-mine the content in such documents, for the purposes of academic research, subject always to the full Conditions of use: [http://www.nature.com/authors/editorial\\_policies/license.html#terms](http://www.nature.com/authors/editorial_policies/license.html#terms)

\*Correspondence: [antonis.rokas@vanderbilt.edu](mailto:antonis.rokas@vanderbilt.edu).

#### Author contributions

Study conception and design: XXS, AR; Acquisition of data: XXS, CTH, AR; Analysis and interpretation of data: XXS, CTH, AR; Drafting of manuscript: XXS, AR; Critical revision: XXS, CTH, AR.

#### Competing interests

The authors declare no competing financial interests.

#### Data availability

All data matrices, all resulting phylogenies, and the custom scripts can be found in the Figshare data repository at DOI: 10.6084/m9.figshare.3792189.

A well-resolved tree of life (ToL) is essential for understanding life's history and the evolution of phenotypic diversity. The genomics revolution has enabled the assembly of many taxon-rich genome-scale data matrices for reconstructing the phylogenies of a wide diversity of lineages across the ToL<sup>1-4</sup>. One important consequence of the large number of loci or genes included in these phylogenomic data matrices is that the internal branches (internodes) in the inferred topologies typically receive very high support values<sup>5-9</sup>, leading to the perception that such branches are definitive and unlikely to change.

However, different phylogenomic analyses can sometimes strongly support branches that contradict one another. For example, concatenation analysis of a 1,233-gene, 96-taxon phylogenomic data matrix (609,899 amino acid sites) provided absolute clade support for the family Ascoideaceae as the closest relative of the families Phaffomycetaceae + Saccharomycodaceae + Saccharomycetaceae<sup>4</sup>; in contrast, concatenation analysis of a 1,559-gene, 38-taxon phylogenomic data matrix (364,126 amino acid sites) robustly placed the family Ascoideaceae as sister to a broader clade composed of the family Pichiaceae, the CUG-Ser clade, the family Phaffomycetaceae, the family Saccharomycodaceae, and the family Saccharomycetaceae<sup>10</sup>. Contradictory branches can even be observed when different analytical approaches are used on the same data matrix. Case in point, a phylogenomic analysis (maximum likelihood, homogeneous model, Opisthokonta as outgroup) of 406 genes from 70 taxa (88,384 amino acid sites) recovered ctenophores as sister to all other metazoan phyla<sup>11</sup>, whereas another analysis (Bayesian inference, heterogeneous model, Choanoflagellata as outgroup) of the same data matrix supported sponges, rather than ctenophores, as the sister to the rest of the metazoan phyla<sup>12</sup>.

While both biological and analytical factors influence phylogenetic inference<sup>13-17</sup>, the first step to understanding why different phylogenomic data matrices (or different analyses of the same data matrix) yield two contradictory topologies is the precise quantification of the phylogenetic signal and identification of the genes or sites that gave rise to such conflict. To address this critical, yet poorly understood, question, we examined the distribution of phylogenetic signal in 17 contentious branches and 6 well-established branches (used as controls), in three large phylogenomic data matrices from plants, animals, and fungi (Table 1). Finally, we applied our approach of dissecting the distribution of phylogenetic signal in eight different phylogenomic data matrices aimed to resolve the controversy regarding the earliest-branching phylum of the Metazoa.

## Results

### Measuring phylogenetic signal

We defined phylogenetic signal as the difference in the log-likelihood scores between two alternative resolutions, T1 and T2, of a given branch (or internode or bipartition) in a phylogenetic tree<sup>18</sup>. For a given data matrix and branch in question, we defined T1 as the bipartition recovered by the phylogenetic tree obtained by maximum likelihood (ML) when the full data matrix is analyzed by concatenation analysis; we defined T2 as a bipartition in the phylogenetic tree that shows substantial topological conflict with T1 (e.g., in most cases, T2 was the most prevalent bipartition conflicting with T1) (Fig. 1a).

To calculate phylogenetic signal, we first calculated the site-wise log-likelihood scores for the unconstrained ML tree under concatenation (by definition, this topology contained the T1 branch and will be hereafter abbreviated T1) as well as for the ML tree constrained to recover the T2 branch (hereafter called T2) under the same substitution model and partitioning strategy (Fig. 1a). Next, we calculated the difference in site-wise log-likelihood scores ( $\Delta$ SLS) between T1 and T2 for every site in a given data matrix. By summing the  $\Delta$ SLS scores of all sites for every gene in a given data matrix, we then obtained the difference in gene-wise log-likelihood scores ( $\Delta$ GLS) between T1 and T2 (Fig. 1b). By doing so, we were able to quantify the distribution of phylogenetic signal for T1 and T2 at the site and gene levels (Fig. 1c), as well as visualize the proportions of sites' or genes' support for T1 and T2 (Fig. 1d). This quantification and visualization of phylogenetic signal can be extended to the comparison of three alternative phylogenetic hypotheses (T1, T2, and T3), as shown in Supplementary Fig. 1.

### A tiny amount of data can drive phylogenetic inference

For each of the 17 contentious branches and the 6 well-established branches (used as controls) in plants, animals, and fungi, we first examined whether the unconstrained ML tree under concatenation (T1) had a significantly different log-likelihood score than the ML tree constrained to recover the T2 branch (T2) using the approximately unbiased (AU) test<sup>19,20</sup>. We found that T2 was significantly worse ( $P$ -value  $< 0.05$ ) than T1 in 22/23 internodes (Table 1); the only exception was the neoavian branch in animals.

Examination of the distribution of  $\Delta$ GLS values (i.e., difference in gene-wise log-likelihood scores between T1 and T2) in the 17 contentious and 6 control branches showed that the proportion of genes supporting T1 was generally greater than that of genes supporting T2 (Fig. 2; Supplementary Figs. 2 and 3a; Supplementary Tables 1–3). The only exceptions were the angiosperm (plants), eutherian (animals), and Ascoideaceae (fungi) branches, where the proportions of genes supporting T1 were slightly smaller than those supporting T2.

Examination of the distribution of  $\Delta$ SLS values (i.e., difference in site-wise log-likelihood scores between T1 and T2) showed that the proportion of sites supporting T1 was greater than that of sites supporting T2 for 18 of the 23 branches (Supplementary Fig. 3b); the remaining 5 branches (eutherian, lungfish, and neoavian in animals, Ascoideaceae and WGD clade in fungi) had lower proportions of sites supporting T1 than T2 (Supplementary Fig. 3b). We observed the same pattern (Supplementary Fig. 4) when we considered only “weak” sites, whose absolute  $\Delta$ SLS values were smaller or equal to 0.5<sup>17</sup>; as more than 95% of sites in each branch were weak ones (Supplementary Table 4), the similarity in results when considering all sites versus only weak sites is not surprising. Comparison of “strong” sites<sup>17</sup>, whose absolute  $\Delta$ SLS values were  $>0.5$ , with all sites for each branch, showed that there was a higher proportion of strong (relative to all) sites favoring T1 in 13 branches and a lower proportion in the other 10 branches. Finally, 3 branches (eutherian and neoavian in animals, Ascoideaceae in fungi) had fewer strong sites supporting T1 than T2 (Supplementary Fig. 4).

Examination of the distribution of GLS values also revealed that, in 6/17 contentious branches, a single or a handful of genes displayed very high GLS values (Fig. 2 and Supplementary Figs. 2, 5–30). Remarkably, we found that removal of the gene with the highest absolute GLS value switched the ML tree's support from T1 to T2 in 3 branches (angiosperm in plants, neoavian in animals, and Ascoideaceae in fungi) (Figs. 2 and 3; Supplementary Figs. 7, 17, and 23). In contrast, random exclusion of a single gene did not change support in any analysis (Fig. 4 and Supplementary Figs. 5, 13, and 22); Similarly, removal of the gene with the highest GLS value in our 6 control branches (Table 1) favored T1 over T2 (Figs. 2–4; Supplementary Figs. 11, 12, 20, 21, 29, and 30).

The single genes whose removal caused the switch of the phylogenomic data matrices' support from T1 to T2 in the angiosperm, neoavian, and Ascoideaceae branches were orthologs of the *Arabidopsis thaliana* *AT3G46220* gene (alignment id: 6040\_C12), the *Homo sapiens* *AUTS2* gene (alignment id: Pro\_ENSG00000158321), and the *Saccharomyces cerevisiae* *DPM1* gene (alignment id: BUSCOFEOG7W9S51), respectively. Plotting of the SLS values (i.e., difference in gene-wise log-likelihood scores between T1 and T2) for the three gene alignments showed that 14.4% of the 6040\_C12 gene alignment, 11.0% of Pro\_ENSG00000158321, and 47.9% of BUSCOFEOG7W9S51 had high SLS values (>0.5); moreover, these strong sites were unevenly distributed in the 6040\_C12 and Pro\_ENSG00000158321 gene alignments (Supplementary Fig. 57). Further examination of the sequence alignments of these three genes did not identify apparently unusual sequences or columns (Supplementary Figs. 58–60), while topological distances (measured by the normalized Robinson–Foulds tree distance, RFD, using RAXML with the option “-f r”) of their ML gene trees from the concatenation-based ML phylogenies (T1) inferred from the full data matrices were slightly higher than the corresponding means of topological distances of all individual gene trees from the concatenation-based ML phylogenies (Supplementary Tables 6–8). Finally, none of the three genes' properties<sup>21</sup> (e.g., alignment length, alignment quality, compositional heterogeneity or disparity index, rate of evolution, single-gene tree resolution [e.g., average bootstrap support]; see Supplementary Table 5) could consistently explain why they exhibited such high GLS values (Supplementary Tables 6–8).

To investigate the impact of model of sequence evolution in the proportions of sites supporting T1 versus T2, we used Seq-Gen v1.3.3<sup>22</sup> to simulate alignments of the plant (290,718 sites), animal (1,806,035 sites) and fungal (609,772 sites) phylogenies using exactly the same ML trees and model parameters (i.e., state frequency, rates, and alpha parameter: the shape for the gamma rate heterogeneity among sites) used in the original three phylogenomic studies as well as in our analyses. Comparison of the differences in the proportions of strong, weak, and all sites supporting T1 between biological and simulated data showed that differences were small for the 6 control branches but much larger for the 17 contentious branches (Supplementary Fig. 61); this trend was especially noticeable when only the strong sites were considered. Furthermore, the differences in the proportion of sites supporting T1 between biological and simulated data were especially pronounced in the angiosperm, neoavian, and Ascoideaceae branches (Supplementary Fig. 61), suggesting that the site- and gene-specific patterns of support for T1 or T2 are a poor fit to those predicted by the employed models of sequence evolution.

To quantify the effect of gene removal, we next investigated the effects of excluding 5, 10, 50, and 100 genes with the highest absolute  $\text{GLS}$  values, as well as of excluding the genes with outlier  $\text{GLS}$  values (see equations (3) and (4) in the Methods section). Our results showed that these gradual removals of genes had the same effect as single gene removal (a switch from T1 to T2) for the angiosperm and Ascoideaceae branches, whereas the neoavian branch was unstable, switching between T1, T2, and other topologies (Fig. 3). Interestingly, the results on single or few gene removals were very similar to the results obtained when outlier genes were removed (Fig. 3). Furthermore, when the number of removed genes was equal or greater than 50, a switch from T1 to T2 or other hypotheses was also observed for the eutherian and neoavian branches in animals and the *Hyphopichia* branch in fungi (Fig. 3).

Coalescence-based species tree approaches<sup>23,24</sup>, by taking into account each gene tree's history, are less likely to be influenced by a single or handful of genes in a phylogenomic data matrix. However, these approaches can be sensitive to errors and biases in estimating individual gene trees<sup>25–27</sup>. To test whether the support for the 17 contentious branches from coalescence-based approaches was, like concatenation, sensitive to the presence of a very small subset of data, we examined the effect of removing the site with the highest absolute  $\text{SLS}$  value from every gene. We found that this removal of a single site per gene altered the topology supported in 9/17 contentious branches (Fig. 4 and Supplementary Figs. 31–56). In contrast, exclusion of a randomly selected single site from every gene did not change support in any analysis (Fig. 4 and Supplementary Figs. 31, 39, and 48); similarly, removal of the single site with the highest absolute  $\text{SLS}$  value per gene in the 6 control branches did not result in a switch of support from T1 to another topology (Fig. 4 and Supplementary Figs. 37, 38, 46, 47, 55, and 56).

Among the branches strongly influenced by the removal of the single site with the highest absolute  $\text{SLS}$  value from every gene were the bryophyte branch in plants, the eutherian, lungfish, neoavian, and teleost branches in animals, and the Ascoideaceae and WGD clade branches in fungi. Interestingly, the neoavian and Ascoideaceae branches were sensitive to both the removal of the gene with the highest absolute  $\text{GLS}$  value and to that of the site with the highest absolute  $\text{SLS}$  value from every gene. Exclusion of the 1% of sites with the highest absolute  $\text{SLS}$  values<sup>28</sup>, from every gene showed that the coalescence-based topology based on the full data matrix was no longer supported for 13/17 contentious branches (Fig. 4 and Supplementary Figs. 31–56).

While some of these 17 contentious relationships appear to be driven by a tiny subset of data and should effectively be considered unresolved, the quantification of  $\text{GLS}$  and  $\text{SLS}$  values for a specific branch of a phylogeny can also augment the support for one of the alternative hypotheses. For example, similar to the well-established branch associated with the monophyly of amniotes on the vertebrate phylogeny that we used as a control (Figs. 2–4), examination of the evolutionary placement of turtles (Table 1 and Figs. 2–4) showed very strong support for the hypothesis that turtles are the sister group to archosaurs (birds + crocodiles). Specifically, the  $\text{GLS}$  values of 74% (3,466 / 4,682) of the genes in the data matrix favor this hypothesis over the second best alternative (turtles as sister group to crocodiles) (Supplementary Fig. 2a); the same is true for  $\text{SLS}$  values (88% or 1,588,738 /

1,806,035 sites favor turtles as the sister group to archosaurs than to just crocodiles; Supplementary Fig. 3b).

### What is the earliest branch of the metazoan phylogeny?

To further illustrate how the quantification of phylogenetic signal for a specific branch of a phylogeny can augment the resolution of contentious branches, we next examined the support for three alternative hypotheses regarding the earliest-branching lineage of the Metazoa (T1: Ctenophora-sister, T2: Porifera-sister, and T3: Porifera+Ctenophora-sister)<sup>11,12,29</sup> (Fig. 5a). Specifically, we collected 8 phylogenomic data matrices from three recent studies<sup>11,29,30</sup>, comprised of different data types (genomic data or “transcriptomic + genomic data”) and different outgroups (Opisthokonta or Choanoflagellata).

Examination of GLS values between T1, T2, and T3 (see Methods for full details) showed that T1 had the highest proportions of supporting genes, ranging from 42.5% to 69.7%, across the 8 data matrices (Fig. 5a and Supplementary Table 9). In addition, the GLS values of genes favoring T1 were higher than those favoring either T2 or T3 across all 8 data matrices (Supplementary Table 9 and Supplementary Fig. 62). This is most easily observed by examining the distribution of ranked GLS values for each data matrix (Supplementary Fig. 63). Moreover, all concatenation ML analyses of the removal of one single gene and the genes with outlier GLS values still supported Ctenophora-sister hypothesis (T1) (Supplementary Figs. 65a–65h).

Examination of SLS values between T1, T2, and T3 (see Methods for full details) showed that T1 also had the highest proportions of supporting sites, ranging from 39.8% to 56.9% (Fig. 5b). Importantly, comparison of the proportions of strong, weak, and all sites supporting T1 showed that this hypothesis received its highest support in all 8 data matrices by the strong sites; their proportions in favor of T1 ranged from 52.2% to 85.3% (Supplementary Fig. 64). Thus, examination of GLS and SLS values in 8 phylogenomic data matrices shows robust support for the Ctenophora-sister hypothesis.

## Discussion

In this study, we examined the distribution and strength of phylogenetic signal on contentious branches of the ToL. For some contentious branches, our approach clarified the nature of the phylogenetic incongruence and, by quantifying the support for alternative hypotheses at the site and gene levels, illuminated their resolution. For other contentious branches, however, we found that tiny amounts of data – in what are otherwise very large phylogenomic data matrices – exerted decisive influence in their resolution.

There are two potential explanations for why this is so. One explanation is that the evolution of these genes may have been shaped by positive selection<sup>31</sup>, which can give rise to convergent evolution that misleads phylogenetic inference<sup>17,32–35</sup>, or by evolutionary processes such as incomplete lineage sorting, horizontal gene transfer, and hybridization, which can give rise to gene histories that differ from each other and from the species history<sup>13,14</sup>. Another, not mutually exclusive, explanation is that the evolutionary history of these genes may have been incorrectly inferred due to the influence of analytical factors,

such as taxon choice<sup>36</sup>, taxon sampling<sup>37</sup>, and misspecification of the model of sequence evolution<sup>15,38</sup> (see also Supplementary Fig. 61). Irrespective of the underlying biological or analytical factors at play, our results on branches sensitive to tiny amounts of data raise doubts about whether these branches are truly resolved.

Our proposed framework for quantifying and visualizing phylogenetic signal could be used to analyze any branch of the tree of life, irrespective of how contentious they are; our examination of 6 control branches (Figs. 2 and 3) is a good case in point. However, our approach is most likely to be useful in cases of branches showing a high degree of conflict (e.g., low scores of internode certainty-related measures<sup>39–41</sup>), or in cases of branches shown to conflict between topologies inferred by different phylogenomic data matrices. For such contentious branches, we would argue that dissecting the distribution of support for each of the main alternative hypotheses is essential for understanding the extent to which they are (or are not) supported by the phylogenomic data<sup>42,43</sup>. Finally, the same analytical approach could be employed to examine the influence of different analytical models (e.g., homogeneous model versus mixture model) on the distribution of phylogenetic signal and the resolution of contentious branches.

Quantifying and visualizing the distribution of phylogenetic signal at the level of sites or genes would also be helpful for the identification of any sites or genes that might be exerting a disproportionate amount of influence on the resolution of a given contentious branch. The undue influence of one or a few genes or a few sites on phylogenetic inference has been previously observed in smaller data matrices<sup>17,28,44–47</sup>. Our results show that this undue influence of one gene or a few sites can, in some cases, be the main reason for the generation of very high support values on a given branch in phylogenomic data matrices that contain several hundreds or thousands of genes. Moreover, both concatenation- and coalescence-based approaches are susceptible to this behavior.

How are we then to interpret inferred relationships that rest on the presence of tiny amounts of data in phylogenomic studies? The history of life abounds with examples of ancient evolutionary radiations. Previous theoretical as well as empirical studies<sup>6,14,48,49</sup> suggest that the resolution of relationships within such series of closely spaced species divergences in deep time can be extremely challenging. It is our view that the branches of the ToL that exhibit this behavior (i.e., their resolution rests on the presence of a tiny subset of genome-scale data) should effectively be considered unresolved. Of course, this does not mean that these branches will never be fully resolved, but rather that we are unable to do with our current methodology and sampling of genes and taxa. Clear demarcation of such unresolved branches would provide a more accurate account of the phylogenetic hypotheses supported by the available data.

## Methods

### Data matrices

We used three taxon- and gene-rich phylogenomic data matrices representing three eukaryotic kingdoms of the tree of life: plants (103 plant species  $\times$  620 nuclear genes; Figure 2 in original study)<sup>1</sup>, animals (58 jawed vertebrate species  $\times$  4,682 nuclear genes; Figure 1 in

original study)<sup>50</sup>, and fungi (86 yeast species × 1,233 nuclear genes; Figure 3 in original study)<sup>4</sup>. Although these studies constructed several different data matrices, we used only the full data matrix in each study.

### Topological hypothesis testing

We investigated a total of 17 contentious branches present in three phylogenomic data matrices from plants, animals, and fungi (Table 1). These branches were deemed contentious either because they were considered as such in the original papers<sup>1,50</sup> or because they were incongruent between the concatenation- and coalescence-based phylogenies<sup>4</sup>. As a control, we also investigated two well-established branches from each of the three phylogenomic data matrices (see Table 1 for full details). For each branch, the unconstrained ML tree under concatenation (T1) and the ML tree constrained to recover the T2 branch were examined (Table 1). In most cases, T2 was the most prevalent bipartition conflicting with T1. The ML tree constrained to recover the T2 branch was obtained by enforcing the topological constraint option (option -g) in RAxML<sup>51</sup>, version 8.2.3. All ML searches were performed by using the same models and partitioning strategies as the original studies; the ML phylogeny was obtained by conducting 5 separate tree searches using 5 different random seeds (option -p). To test whether the T2 topology was statistically worse than the T1 topology for each of the 17 branches, we applied the approximately unbiased (AU)<sup>19</sup> test in the software package CONSEL<sup>20</sup>, version 0.20. The AU test was conducted using the multi-scale bootstrap technique based on the site-wise log-likelihood scores, which were calculated in RAxML (option -f G). Notably, the difference between the RAxML software<sup>51</sup>, version 8.2.3, and the IQ-TREE software<sup>52</sup>, version 1.5.1, in calculating log-likelihood scores for our 17 contentious branches was very small (Supplementary Table 10).

### Phylogenetic signal

A schematic workflow for the calculation and visualization of phylogenetic signal is shown in Fig. 1. For a given data matrix and branch in question, we defined T1 as the bipartition recovered by the phylogenetic tree obtained by maximum likelihood (ML) when the full data matrix is analyzed by concatenation analysis; we defined T2 as a bipartition in the phylogenetic tree that shows substantial topological conflict with T1 (e.g., in most cases, T2 was the most prevalent bipartition conflicting with T1) (Fig. 1a). For a given data matrix and branch in question, using the maximum likelihood framework<sup>18</sup>, we here defined phylogenetic signal as the difference in the log-likelihood scores for the unconstrained ML tree under concatenation (by definition, this tree contained the T1 branch) against the ML tree constrained to recover the T2 branch (T2). Briefly, we first estimated the site-wise log-likelihood values for both T1 and T2 based on the concatenation data matrix and the same models using RAxML (option -f G). We then calculated the difference in site-wise log-likelihood scores (SLS) between T1 and T2 using the equation:

$$\Delta SLS_i = \ln L(S_i|T1) - \ln L(S_i|T2) \quad (1)$$

where T1 is the unconstrained ML tree obtained by concatenation analysis of the full data matrix and T2 the ML tree constrained to recover the T2 branch. SLS<sub>i</sub> is the difference in



site-wise log-likelihood scores under T1 and T2 for the  $i$ th site ( $S_i$ ) in the full data matrix. Similarly, we also calculated the difference in gene-wise log-likelihood scores ( $\Delta GLS$ ) for T1 versus T2 for every gene according to:

$$\Delta GLS_j = \ln L(G_j|T1) - \ln L(G_j|T2) \quad (2)$$

where T1 is the unconstrained ML tree obtained by concatenation analysis of the full data matrix and T2 the ML tree constrained to recover the T2 branch.  $\Delta GLS_j$  is difference in gene-wise log-likelihood scores under T1 and T2 and can be calculated as the sum of  $\Delta GLS$  values of all sites within the  $j$ th gene ( $G_j$ ).

### Effect of removing a tiny amount of data on phylogenetic inference

To examine the influence of tiny amounts of data on phylogenetic inference, we generated 6 reduced data matrices by excluding 1, 5, 10, 50, and 100 genes with the highest absolute  $\Delta GLS$  values (i.e., difference in gene-wise log-likelihood scores between T1 and T2), as well as all genes whose  $\Delta GLS$  values were outliers, from the full data matrix for each of the 17 contentious branches and 6 well-established control branches. Outlier genes were defined as those whose absolute  $\Delta GLS$  values were greater than the upper whisker or smaller than the lower whisker of a boxplot in R<sup>53</sup>,

$$Upper\ whisker = \min(\max(x), Q3 + 1.5 * IQR) \quad (3)$$

$$Lower\ whisker = \max(\min(x), Q1 - 1.5 * IQR) \quad (4)$$

where  $\max(x)$  and  $\min(x)$  are the maximum value and minimum value for a set of absolute  $\Delta GLS$  values, respectively. Q1 and Q3 are the first quartile and the third quartile, respectively. IQR (interquartile range) is difference in value between Q3 and Q1 ( $Q3 - Q1$ ).

As a control, we also randomly excluded a single gene from the full data matrix and repeated this process 5 times in each of the three data matrices. For each reduced data matrix (we examined a total of 153 data matrices), the ML tree was inferred, as implemented in the IQ-TREE software<sup>52</sup> using the same substitution models (plant: GTR+GAMMA; animal: LG+GAMMA+F; fungi: LG+GAMMA) and partitioning strategies (plant: 8 partitions; animal: 1 partition; fungi: 1 partition) as described in the original papers. Branch support for each internode was evaluated with 100 rapid bootstrapping replicates<sup>54</sup> using RAxML<sup>51</sup> (option -x). Since the bootstrapping analysis of such large data matrices in RAxML is computationally very expensive (each plant data matrix takes ~150 CPU hours; each animal data matrix takes ~4,200 CPU hours; each fungal data matrix takes ~2,900 CPU hours), we performed bootstrapping on only two (those associated with removal of a single gene and removal of all outlier genes) of the 6 reduced data matrices for each of the 17 contentious branches and 6 well-established branches.

Similarly, we excluded the site with the highest absolute  $\Delta SLS$  value (i.e., the difference in site-wise log-likelihood scores between T1 and T2) from every gene for each branch. As a control, we also created reduced individual gene alignments where one site was randomly excluded for each data matrix. Maximum likelihood analysis of each reduced individual gene alignment was performed in RAxML by conducting 100 rapid bootstrapping replicates and 10 separate ML searches. Finally, the resulting RAxML ML trees and their 100 rapid bootstrapping trees were used to infer the coalescence-based species phylogeny with the ASTRAL software<sup>55</sup>, version 2.4.7.7. In addition to removal of a single site with the highest absolute  $\Delta SLS$  value, we also excluded the 1% of sites with the highest absolute  $\Delta GLS$  values from every gene for each branch, as implemented in Shavit Grievink et al.<sup>28</sup>.

### The root of the Metazoan phylogeny

To investigate the distribution of phylogenetic signal in studies aiming to elucidate which was the first-branching metazoan phylum<sup>11,12,29,30,56–61</sup>, we considered 8 data matrices from three recent studies that were constructed from either EST and genomic data<sup>11</sup>, transcriptomic and genomic data<sup>29</sup>, or genomic data alone<sup>30</sup>. Because different choices of outgroups could influence phylogenetic inference<sup>9,12</sup>, we investigated the distribution of phylogenetic signal in data matrices that used two different types of outgroups: Choanoflagellata, the closest relative of the metazoan phyla, and non-metazoan Opisthokonta, which included fungi and non-metazoan holozoans, such as choanoflagellates.

We examined 3 hypotheses: Ctenophora-sister (T1; Fig. 5a), Porifera-sister (T2; Fig. 5a), and Porifera + Ctenophora-sister (T3; Fig. 5a). For each hypothesis, its corresponding constraint ML phylogeny and its site-wise log-likelihood scores were estimated for each of 8 data matrices using RAxML, as described above. We then calculated the mean of all pairwise absolute differences in site-wise log-likelihood scores ( $\Delta SLS_i$ ) between T1, T2, and T3 for the  $i$ th site ( $S_i$ ) in the full data matrix using the equation (5):

$$\Delta SLS_i = \frac{|lnL(S_i|T1) - lnL(S_i|T2)| + |lnL(S_i|T1) - lnL(S_i|T3)| + |lnL(S_i|T2) - lnL(S_i|T3)|}{3}$$

(5)

Similarly, we calculated the mean of all pairwise absolute differences in gene-wise log-likelihood scores ( $\Delta GLS_j$ ) between T1, T2, and T3 (see Supplementary Fig. 1 for full schematic representation) using the equation (6):

$$\Delta GLS_j = \frac{|lnL(G_j|T1) - lnL(G_j|T2)| + |lnL(G_j|T1) - lnL(G_j|T3)| + |lnL(G_j|T2) - lnL(G_j|T3)|}{3}$$

(6)

Last, we examined whether removal of a single gene with the highest absolute GLS value or removal of the genes with outlier GLS values [see equations (3) and (4)] altered the hypothesis favored by concatenation analysis.

## Supplementary Material

Refer to Web version on PubMed Central for supplementary material.

## Acknowledgments

We thank members of the Rokas lab, and in particular Xiaofan Zhou, for helpful discussions and comments. We also thank Mengyun Chen for kindly providing the animal phylogenomic data matrix, Jim Leebens-Mack for providing further information about the plant data matrix, as well as four referees for insightful comments that improved this work. This work was conducted in part using the resources of the Advanced Computing Center for Research and Education (ACCRE) at Vanderbilt University, of the UW-Madison Center for High Throughput Computing, and of the CIPRES Science Gateway<sup>62</sup>. This work was supported by the National Science Foundation (DEB-1442113 to AR; DEB-1442148 to CTH), in part by the DOE Great Lakes Bioenergy Research Center (DOE Office of Science BER DE-FC02-07ER64494), the USDA National Institute of Food and Agriculture (Hatch project 1003258 to CTH), and the National Institutes of Health (NIAID AI105619 to AR). CTH is a Pew Scholar in the Biomedical Sciences, supported by the Pew Charitable Trusts.

## References

1. Wickett NJ, et al. Phylotranscriptomic analysis of the origin and early diversification of land plants. *Proc Natl Acad Sci USA*. 2014; 111:E4859–E4868. [PubMed: 25355905]
2. Misof B, et al. Phylogenomics resolves the timing and pattern of insect evolution. *Science*. 2014; 346:763–767. [PubMed: 25378627]
3. Jarvis ED, et al. Whole-genome analyses resolve early branches in the tree of life of modern birds. *Science*. 2014; 346:1320–1331. [PubMed: 25504713]
4. Shen X-X, et al. Reconstructing the Backbone of the Saccharomycotina Yeast Phylogeny Using Genome-Scale Data. *G3*. 2016; 6:3927–3939. [PubMed: 27672114]
5. Rokas A, Williams BL, King N, Carroll SB. Genome-scale approaches to resolving incongruence in molecular phylogenies. *Nature*. 2003; 425:798–804. [PubMed: 14574403]
6. Rokas A, Carroll SB. Bushes in the Tree of Life. *PLoS Biol*. 2006; 4:e352. [PubMed: 17105342]
7. Delsuc F, Brinkmann H, Philippe H. Phylogenomics and the reconstruction of the tree of life. *Nat Rev Genet*. 2005; 6:361–375. [PubMed: 15861208]
8. Philippe H, Delsuc F, Brinkmann H, Lartillot N. Phylogenomics. *Annu Rev Ecol Evol Syst*. 2005; 36:541–562.
9. Philippe H, et al. Resolving Difficult Phylogenetic Questions: Why More Sequences Are Not Enough. *PLoS Biol*. 2011; 9:e1000602. [PubMed: 21423652]
10. Riley R, et al. Comparative genomics of biotechnologically important yeasts. *Proc Natl Acad Sci USA*. 2016; 113:9882–9887. [PubMed: 27535936]
11. Ryan JF, et al. The genome of the ctenophore *Mnemiopsis leidyi* and its implications for cell type evolution. *Science*. 2013; 342:1242592. [PubMed: 24337300]
12. Pisani D, et al. Genomic data do not support comb jellies as the sister group to all other animals. *Proc Natl Acad Sci USA*. 2015; 112:15402–15407. [PubMed: 26621703]
13. Nakhleh L. Computational approaches to species phylogeny inference and gene tree reconciliation. *Trends Ecol Evol*. 2013; 28:719–728. [PubMed: 24094331]
14. Degnan JH, Rosenberg NA. Gene tree discordance, phylogenetic inference and the multispecies coalescent. *Trends Ecol Evol*. 2009; 24:332–340. [PubMed: 19307040]
15. Phillips MJ, Delsuc F, Penny D. Genome-scale phylogeny and the detection of systematic biases. *Mol Biol Evol*. 2004; 21:1455–1458. [PubMed: 15084674]
16. Hess J, Goldman N. Addressing Inter-Gene Heterogeneity in Maximum Likelihood Phylogenomic Analysis: Yeasts Revisited. *PLoS One*. 2011; 6:e22783. [PubMed: 21850235]

17. Castoe TA, et al. Evidence for an ancient adaptive episode of convergent molecular evolution. *Proc Natl Acad Sci USA*. 2009; 106:8986–8991. [PubMed: 19416880]
18. Felsenstein J. Evolutionary trees from DNA sequences: a maximum likelihood approach. *J Mol Evol*. 1981; 17:368–376. [PubMed: 7288891]
19. Shimodaira H. An approximately unbiased test of phylogenetic tree selection. *Syst Biol*. 2002; 51:492–508. [PubMed: 12079646]
20. Shimodaira H, Hasegawa M. CONSEL: for assessing the confidence of phylogenetic tree selection. *Bioinformatics*. 2001; 17:1246–1247. [PubMed: 11751242]
21. Shen X-X, Salichos L, Rokas A. A Genome-Scale Investigation of How Sequence, Function, and Tree-Based Gene Properties Influence Phylogenetic Inference. *Genome Biol Evol*. 2016; 8:2565–2580. [PubMed: 27492233]
22. Rambaut A, Grassly NC. Seq-Gen: an application for the Monte Carlo simulation of DNA sequence evolution along phylogenetic trees. *Comput Appl Biosci*. 1997; 13:235–238. [PubMed: 9183526]
23. Rannala B, Yang Z. Bayes estimation of species divergence times and ancestral population sizes using DNA sequences from multiple loci. *Genetics*. 2003; 164:1645–1656. [PubMed: 12930768]
24. Edwards SV. Is a new and general theory of molecular systematics emerging? *Evolution*. 2009; 63:1–19. [PubMed: 19146594]
25. Mirarab S, Bayzid MS, Boussau B, Warnow T. Statistical binning enables an accurate coalescent-based estimation of the avian tree. *Science*. 2014; 346:1250463–1250463. [PubMed: 25504728]
26. Springer MS, Gatesy J. The gene tree delusion. *Mol Phylogenet Evol*. 2016; 94:1–33. [PubMed: 26238460]
27. Liu L, Xi Z, Davis CC. Coalescent Methods Are Robust to the Simultaneous Effects of Long Branches and Incomplete Lineage Sorting. *Mol Biol Evol*. 2015; 32:791–805. [PubMed: 25431481]
28. Shavit Grievink L, Penny D, Holland BR. Missing data and influential sites: choice of sites for phylogenetic analysis can be as important as taxon sampling and model choice. *Genome Biol Evol*. 2013; 5:681–687. [PubMed: 23471508]
29. Whelan N, Kocot KM, Moroz LL, Halanych KM. Error, signal, and the placement of Ctenophora sister to all other animals. *Proc Natl Acad Sci USA*. 2015; 112:5773–5778. [PubMed: 25902535]
30. Borowiec ML, Lee EK, Chiu JC, Plachetzki DC. Extracting phylogenetic signal and accounting for bias in whole-genome data sets supports the Ctenophora as sister to remaining Metazoa. *BMC Genomics*. 2015; 16:987. [PubMed: 26596625]
31. Yang Z. Likelihood ratio tests for detecting positive selection and application to primate lysozyme evolution. *Mol Biol Evol*. 1998; 15:568–573. [PubMed: 9580986]
32. Foote AD, et al. Convergent evolution of the genomes of marine mammals. *Nat Genet*. 2015; 47:272–275. [PubMed: 25621460]
33. Stern DL. The genetic causes of convergent evolution. *Nat Rev Genet*. 2013; 14:751–764. [PubMed: 24105273]
34. Hahn MW, Nakhleh L. Irrational exuberance for resolved species trees. *Evolution*. 2016; 70:7–17. [PubMed: 26639662]
35. Li Y, Liu Z, Shi P, Zhang J. The hearing gene *Prestin* unites echolocating bats and whales. *Curr Biol*. 2010; 20:R55–R56. [PubMed: 20129037]
36. Rokas A, Carroll SB. More genes or more taxa? The relative contribution of gene number and taxon number to phylogenetic accuracy. *Mol Biol Evol*. 2005; 22:1337–1344. [PubMed: 15746014]
37. Heath TA, Hedtke SM, Hillis DM. Taxon sampling and the accuracy of phylogenetic analyses. *J Syst Evol*. 2008; 46:239–257.
38. Goldstein RA, Pollard ST, Shah SD, Pollock DD. Nonadaptive Amino Acid Convergence Rates Decrease over Time. *Mol Biol Evol*. 2015; 32:1373–1381. [PubMed: 25737491]
39. Salichos L, Rokas A. Inferring ancient divergences requires genes with strong phylogenetic signals. *Nature*. 2013; 497:327–331. [PubMed: 23657258]

40. Salichos L, Stamatakis A, Rokas A. Novel information theory-based measures for quantifying incongruence among phylogenetic trees. *Mol Biol Evol.* 2014; 31:1261–1271. [PubMed: 24509691]
41. Kobert K, Salichos L, Rokas A, Stamatakis A. Computing the Internode Certainty and Related Measures from Partial Gene Trees. *Mol Biol Evol.* 2016; 33:1606–1617. [PubMed: 26915959]
42. Tarver JE, et al. The Interrelationships of Placental Mammals and the Limits of Phylogenetic Inference. *Genome Biol Evol.* 2016; 8:330–344. [PubMed: 26733575]
43. Takezaki N, Nishihara H. Resolving the Phylogenetic Position of Coelacanth: The Closest Relative Is Not Always the Most Appropriate Outgroup. *Genome Biol Evol.* 2016; 8:1208–1221. [PubMed: 27026053]
44. Kimball RT, Wang N, Heimer-McGinn V, Ferguson C, Braun EL. Identifying localized biases in large datasets: a case study using the avian tree of life. *Mol Phylogenet Evol.* 2013; 69:1021–1032. [PubMed: 23791948]
45. Gatesy J, et al. Resolution of a concatenation/coalescence kerfuffle: partitioned coalescence support and a robust family-level tree for Mammalia. *Cladistics.* 2016; doi: 10.1111/cla.12170
46. Bar-Hen A, Mariadassou M, Poursat M-A, Vandenkoornhuysen P. Influence Function for Robust Phylogenetic Reconstructions. *Mol Biol Evol.* 2008; 25:869–873. [PubMed: 18263606]
47. Brown JM, Thomson RC. Bayes factors unmask highly variable information content, bias, and extreme influence in phylogenomic analyses. *Syst Biol.* 2016; doi: 10.1093/sysbio/syw101
48. Mossel, E., Steel, M. Mathematics of evolution and phylogeny. Gascuel, O., editor. Oxford University Press; 2005. p. 384-412.
49. Whitfield JB, Lockhart PJ. Deciphering ancient rapid radiations. *Trends Ecol Evol.* 2007; 22:258–265. [PubMed: 17300853]
50. Chen M-Y, Liang D, Zhang P. Selecting Question-Specific Genes to Reduce Incongruence in Phylogenomics: A Case Study of Jawed Vertebrate Backbone Phylogeny. *Syst Biol.* 2015; 64:1104–1120. [PubMed: 26276158]
51. Stamatakis A. RAxML version 8: A tool for phylogenetic analysis and post-analysis of large phylogenies. *Bioinformatics.* 2014; 30:1312–1313. [PubMed: 24451623]
52. Nguyen L-T, Schmidt HA, von Haeseler A, Minh BQ. IQ-TREE: A Fast and Effective Stochastic Algorithm for Estimating Maximum-Likelihood Phylogenies. *Mol Biol Evol.* 2015; 32:268–274. [PubMed: 25371430]
53. Ihaka R, Gentleman R. R: a language for data analysis and graphics. *J Comput Graph Stat.* 1996; 5:299–314.
54. Stamatakis A, Hoover P, Rougemont J. A rapid bootstrap algorithm for the RAxML Web servers. *Syst Biol.* 2008; 57:758–771. [PubMed: 18853362]
55. Mirarab S, Warnow T. ASTRAL-II: coalescent-based species tree estimation with many hundreds of taxa and thousands of genes. *Bioinformatics.* 2015; 31:i44–i52. [PubMed: 26072508]
56. Dunn CW, et al. Broad phylogenomic sampling improves resolution of the animal tree of life. *Nature.* 2008; 452:745–749. [PubMed: 18322464]
57. Hejnol A, et al. Assessing the root of bilaterian animals with scalable phylogenomic methods. *Proc R Soc B Biol Sci.* 2009; 276:4261–4270.
58. Moroz LL, et al. The ctenophore genome and the evolutionary origins of neural systems. *Nature.* 2014; 510:109–114. [PubMed: 24847885]
59. Philippe H, et al. Phylogenomics revives traditional views on deep animal relationships. *Curr Biol.* 2009; 19:706–712. [PubMed: 19345102]
60. Pick KS, et al. Improved phylogenomic taxon sampling noticeably affects nonbilaterian relationships. *Mol Biol Evol.* 2010; 27:1983–1987. [PubMed: 20378579]
61. Nosenko T, et al. Deep metazoan phylogeny: When different genes tell different stories. *Mol Phylogenet Evol.* 2013; 67:223–233. [PubMed: 23353073]
62. Miller, MA., Pfeiffer, W., Schwartz, T. Proceedings of the Gateway Computing Environments Workshop (GCE). IEEE; 2010. Creating the CIPRES Science Gateway for inference of large phylogenetic trees; p. 1-8.

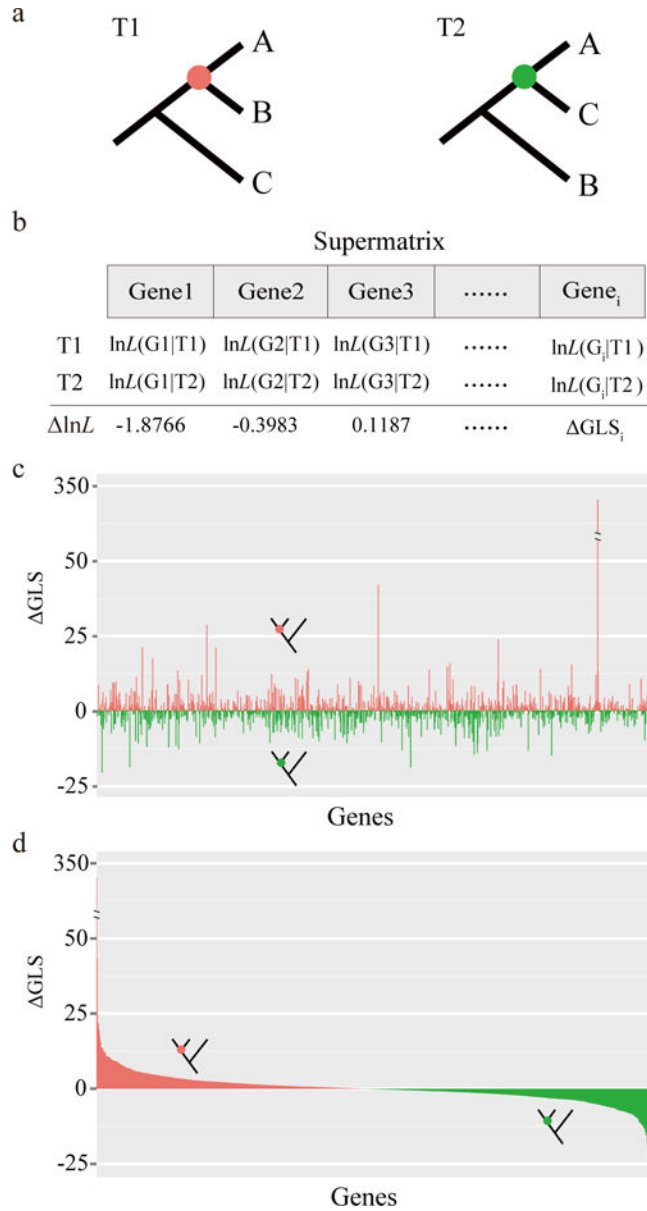


**Figure 1. A schematic representation of our approach for quantifying and visualizing phylogenetic signal in a phylogenomic data matrix**

a, Two alternative phylogenetic hypotheses (T1, the unconstrained ML tree under concatenation; T2, the ML tree constrained to recover the T2 branch). b, Calculation of the difference in the gene-wise log-likelihood scores ( $\Delta GLS$ ) of T1 versus T2 for each gene in the data matrix. The difference in the site-wise log-likelihood scores,  $\Delta SLS$ , of T1 versus T2 for each site in the data matrix is also calculated but is not shown here. The gene-wise phylogenetic signal ( $\Delta GLS$ ) for T1 versus T2 can be visualized either by arranging genes in the order of their placements in the data matrix (c) or in descending order of their  $\Delta GLS$  values (d). Red bars denote genes supporting T1, whereas green bars denote genes supporting T2. The data for panels c and d are the actual values from the analysis of the Ascoideaceae branch in the fungal phylogenomic data matrix (Table 1). The schematic

representation of our approach for quantifying and visualizing phylogenetic signal among three alternative phylogenetic hypotheses (T1, T2, and T3) is shown in Supplementary Fig. 1.

Author Manuscript

Author Manuscript

Author Manuscript

Author Manuscript

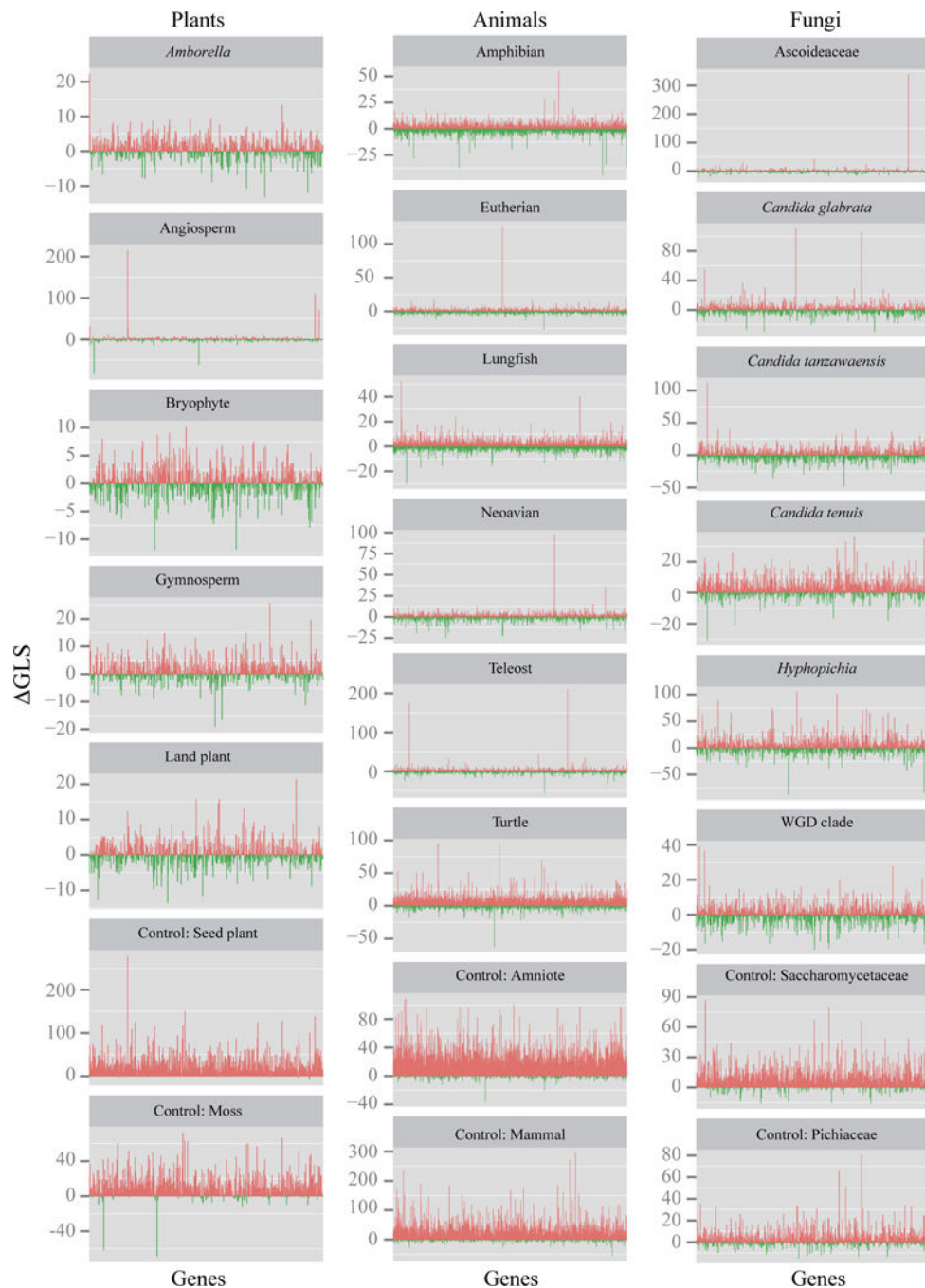


**Figure 2. Distributions of phylogenetic signal for 17 contentious branches in plant, animal, and fungal phylogenomic data matrices**

For each branch,  $\Delta$ GLS values (Y-axis) were calculated by measuring the difference in gene-wise log-likelihood scores for T1 versus T2. The distribution of  $\Delta$ GLS values was visualized by displaying their values for all genes in the phylogenetic data matrix in the order of their placement in the matrix (X-axis; see Supplementary Table 1–3). As a control, we also examined the distribution of  $\Delta$ GLS values for two well-established branches for each of the three data matrices (Plants, monophyly of seed plants and monophyly of mosses; Animals, monophyly of amniotes and monophyly of mammals; Fungi, monophyly of the family



Saccharomycetaceae and paraphyly of the family Pichiaceae; Table 1). Red bars denote genes supporting T1, whereas green bars denote genes supporting T2. The distributions of ranked GLS values for these 23 branches are provided in Supplementary Fig. 2. The specific T1 and T2 topologies compared in each of the branches examined are provided in Table 1.

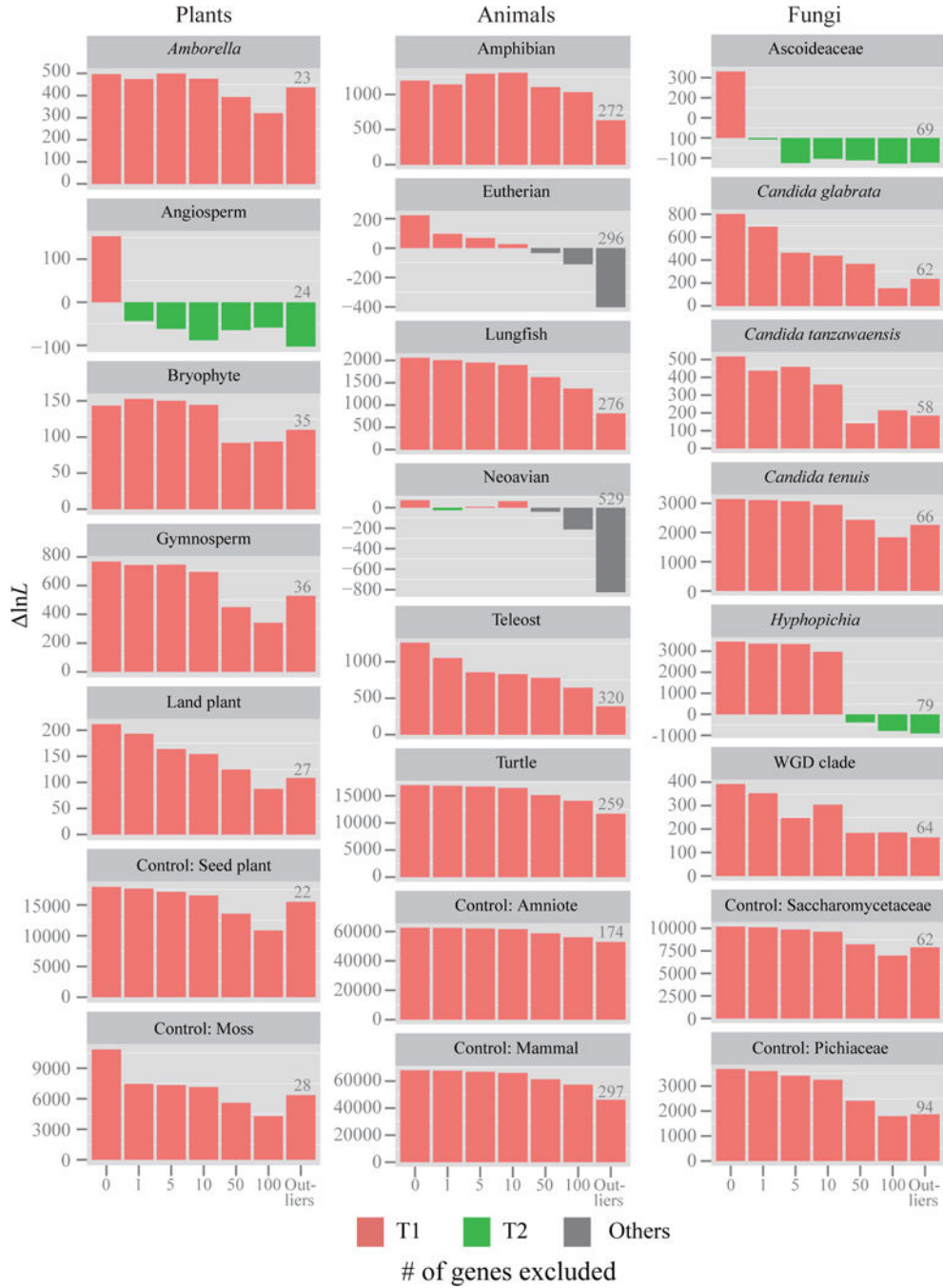


**Figure 3. Quantification of the effect of the removal of tiny amounts of data on the branch’s topology for 17 contentious branches in plant, animal, and fungal phylogenomic data matrices** For each branch, the 1, 5, 10, 50, and 100 genes with the highest absolute GLS values were excluded; we also excluded the genes with outlier GLS values (the number of outlier genes is given above the corresponding bar for each branch). The Y-axis shows the difference in log-likelihood scores ( $\Delta \ln L$ ) for the favored topological hypothesis. The different hypotheses favored are indicated by different bar colors; red bars denotes that ML trees inferred from their corresponding data matrices support T1; green bars denote ML trees supporting T2; gray bars denote ML trees supporting hypotheses other than T1 and T2. The  $\Delta \ln L$  values

displayed on the Y-axis corresponds to the difference in log-likelihood values for T1 against either T2 or “others”. If  $\ln L$  is  $> 0$ , then the ML tree supports T1, whereas if  $\ln L$  is  $< 0$ , then ML tree supports T2 or “others”.

Author Manuscript

Author Manuscript

Author Manuscript

Author Manuscript

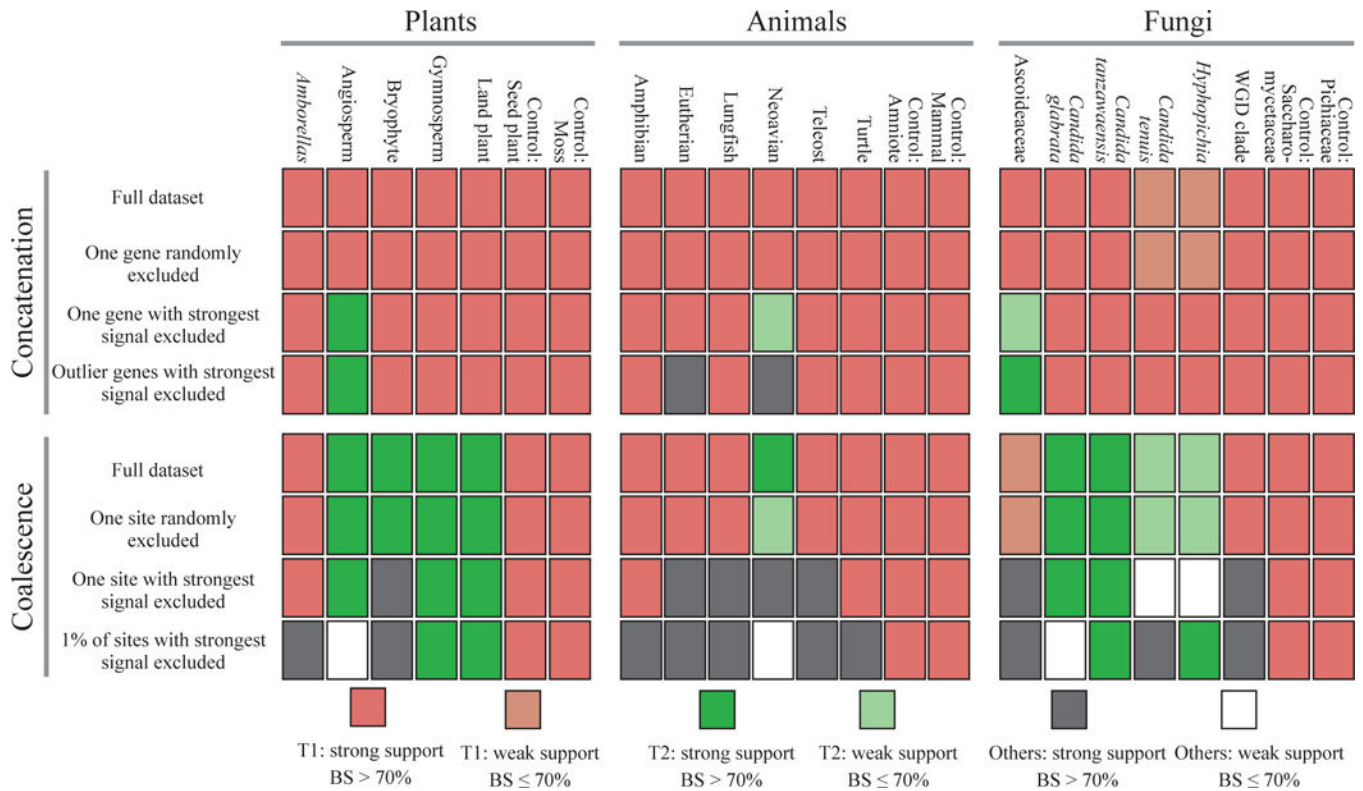


**Figure 4. Tiny amounts of data exert decisive influence in the resolution of certain contentious branches in phylogenomic studies**

The effect of the removal of tiny amounts of data on the branch's topology and bootstrap support (BS) was quantified for 17 contentious branches and 6 well-established branches (controls) in plant, animal, and fungal phylogenomic data matrices. Different colors indicate different branch topologies and levels of BS. Topologies other than T1 and T2 are collectively referred to as "Others". (Top panel: Concatenation) The first row depicts the results of the concatenation analysis when the full data matrix is used, the second row when a single random gene is excluded, the third row when the gene with the highest absolute GLS value is excluded, and the fourth row when the genes with outlier GLS values are excluded. (Bottom panel: Coalescence) The first row depicts the results of the coalescence-based analysis when the full data matrix is used, the second row when one random site from every gene's alignment is excluded, the third row when the site with the highest absolute SLS value from every gene is excluded, and the fourth row when the 1% of sites with the highest absolute SLS values from every gene are excluded. All topologies summarized in this figure are provided in Supplementary Figs. 5–56.

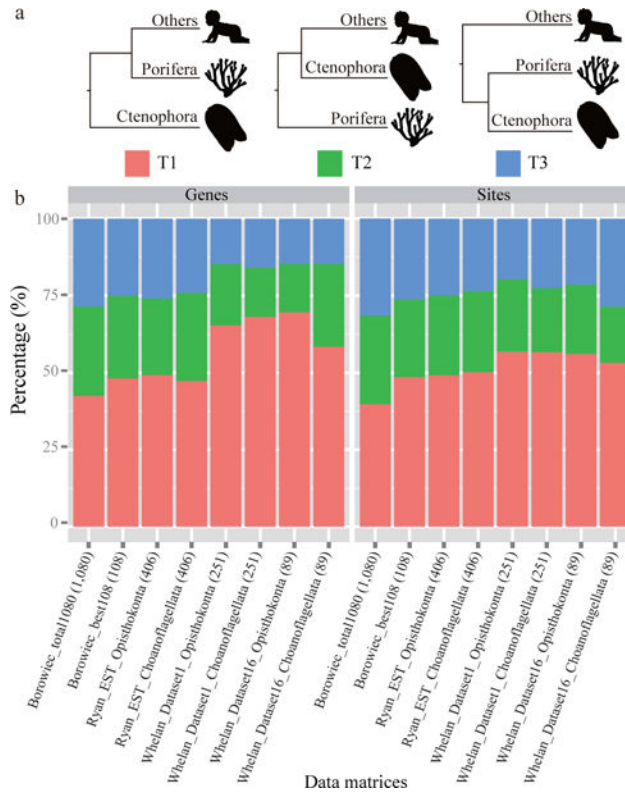


**Figure 5. The distribution of phylogenetic signal for three alternative topological hypotheses on the earliest-branching metazoan lineage**

a, The three alternative topological hypotheses are: ctenophores as the sister group to all other metazoan phyla (Ctenophora-sister) (T1), sponges as the sister group to all other metazoans (Porifera-sister) (T2), or a clade composed of ctenophores and sponges as the sister group to all other metazoans (Porifera+Ctenophora-sister) (T3). All silhouettes come from <http://phylopic.org>. Human image by Andrew Farke, ctenophore and sponge images by Mali’o Kodis, adapted from photograph by Derek Keats (<http://www.flickr.com/photos/dkeats/>). b, Proportions of genes or sites supporting each of three alternative hypotheses for each of eight data matrices from three phylogenomic studies<sup>11,29,30</sup>. Note that two different non-animal outgroup sets are used in the studies by Ryan et al.<sup>11</sup> and by Whelan et al.<sup>29</sup>: datasets whose labels include the word “Choanoflagellata” use only choanoflagellate taxa as outgroups, whereas datasets labeled with “Opisthokonta” use fungal, holozoan taxa, including choanoflagellates, as outgroups. Values in parentheses next to data matrices’ names indicate the number of genes present in each phylogenomic data matrix. The GLS values for the genes across each data matrix are provided in Supplementary Table 9 and their distributions are shown in Supplementary Figs. 62 and 63. The phylograms of all concatenation ML analyses following the removal of the gene with the highest GLS value as well as those following the removal of the genes with outlier GLS values in the eight data matrices can be found in Supplementary Figs. 65a–65h.

**Table 1**

The 17 contentious branches and 6 well-established branches (controls) as well as their alternative hypotheses in three phylogenomic data matrices from plants, animals, and fungi.

Kingdom	Branch	Maximum likelihood tree (T1)	Alternative hypothesis (T2)	P-value of AU& test
Plants	<i>Amborella</i>	<i>Amborella</i> as sister to all other flowering plants	<i>Amborella</i> + <i>Nuphar</i> as sister to all other flowering plants	0.001*
	Angiosperm	Magnoliids as sister to Eudicots + Chloranthales	Magnoliids + Chloranthales as sister to Eudicots	0.030*
	Bryophyte	Hornworts as sister to all other land plants	Hornworts as sister to mosses + liverworts	0.012*
	Gymnosperm	Gnetales as sister to the Pinaceae, nested within the Coniferales	Gnetales as sister to the Coniferales	2e-06*
	Land plant	Zygnematophyceae as sister to all land plants	Charales as sister to all land plants	0.003*
	Control: Seed plant	Seed plants are monophyletic	Seed plants are paraphyletic	3e-99*
	Control: Moss	Mosses are monophyletic	Mosses are paraphyletic	1e-43*
Animals	Amphibian	Gymnophiona as sister to all other amphibians	Anura as sister to all other amphibians	6e-13*
	Eutherian	Xenarthra + Afrotheria as sister to all other placental mammals	Afrotheria as sister to all other placental mammals	0.036*
	Lungfish	Lungfishes as sister to all tetrapods	Lungfishes + coelacanths as sister to all tetrapods	7e-41*
	Neoavian	Pigeons as sister to all other Neoaves	Falcons as sister to all other Neoaves	0.322
	Teleost	Elopomorpha + Osteoglossomorpha as sister to all other teleosts	Osteoglossomorpha alone as sister to all other teleosts	2e-05*
	Turtle	Turtles as sister to archosaurs (birds + crocodiles)	Turtles as sister to crocodiles	1e-29*
	Control: Amniote	Amniotes are monophyletic	Amniotes are paraphyletic	2e-05*
Control: Mammal	Mammals are monophyletic	Mammals are paraphyletic	1e-06*	
Fungi	Ascoideaceae	Ascoideaceae as sister to Phaffomycetaceae + Saccharomycodaceae + Saccharomycetaceae	Ascoideaceae as sister to Pichiaceae + CUG-Ser clade + Phaffomycetaceae + Saccharomycodaceae + Saccharomycetaceae	0.005*
	<i>Candida glabrata</i>	<i>Candida glabrata</i> + <i>Nakaseomyces</i> as sister to <i>Saccharomyces</i>	<i>Kazachstania</i> + <i>Naumovozya</i> as sister to <i>Saccharomyces</i>	1e-07*
	<i>Candida tanzawaensis</i>	<i>Candida tanzawaensis</i> as sister to <i>Scheffersomyces stipitis</i> + <i>Candida</i>	<i>Candida tanzawaensis</i> + <i>Scheffersomyces stipitis</i> as sister to <i>Candida</i>	0.012*
	<i>Candida tenuis</i>	<i>Candida tenuis</i> as sister to all other CUG-Ser yeasts	<i>Candida tenuis</i> as sister to <i>Debaryomyces</i> + <i>Meyerozyma</i> + <i>Candida</i>	2e-59*
	<i>Hyphopichia</i>	<i>Hyphopichia burtonii</i> as sister to <i>Candida auris</i> + <i>Metschnikowia</i>	<i>Hyphopichia burtonii</i> as sister to <i>Debaryomyces</i> + <i>Meyerozyma</i>	1e-53*
	WGD clade	Yeasts of the WGD clade are monophyletic	Yeasts of the WGD clade are paraphyletic	0.002*
	Control: Saccharomycetaceae	Yeasts of the family Saccharomycetaceae are monophyletic	Yeasts of the family Saccharomycetaceae are paraphyletic	2e-05*
Control: Pichiaceae	Yeasts of the family Pichiaceae are paraphyletic	Yeasts of the family Pichiaceae are monophyletic	7e-05*	

& For each branch, the topological test between T1 and T2 was conducted using the approximately unbiased (AU)<sup>19</sup> test, as implemented in the CONSEL software, version 2.0<sup>20</sup>, with 1000 bootstrap replicates. Star symbols (\*) indicate cases where T1 is significantly better than T2 (P-value < 0.05).

Author Manuscript

Author Manuscript

Author Manuscript

Author Manuscript